SCIENTIFIC REPORTS

OPEN

Energy gaps in $Bi_2Sr_2CaCu_2O_{8+\delta}$ cuprate superconductors

J. K. Ren, X. B. Zhu, H. F. Yu, Ye Tian, H. F. Yang, C. Z. Gu, N. L. Wang, Y. F. Ren & S. P. Zhao

Beijing National Laboratory for Condensed Matter Physics, Institute of Physics, Chinese Academy of Sciences, Beijing 100190, China.

SUBJECT AREAS:
SUPERCONDUCTIVITY
ELECTRONIC MATERIALS AND DEVICES
SUPERCONDUCTING MATERIALS
MATERIALS PHYSICS

Received
9 June 2011

Accepted
20 January 2012

Published
6 February 2012

Correspondence and requests for materials should be addressed to S.P.Z. (spzhao@aphy.iphy.ac.cn)

The relationship between the cuprate pseudogap (Δ_p) and superconducting gap (Δ_s) remains an unsolved mystery. Here, we present a temperature- and doping-dependent tunneling study of submicron $Bi_2Sr_2CaCu_2O_{8+\delta}$ intrinsic Josephson junctions, which provides a clear evidence that Δ_s closes at a temperature T_{c0} well above the superconducting transition temperature T_c but far below the pseudogap opening temperature T^*. We show that the superconducting pairing first occurs predominantly on a limited Fermi surface near the node below T_{c0}, accompanied by a Fermi arc due to the lifetime effects of quasiparticles and Cooper pairs. The arc length has a linear temperature dependence, and as temperature decreases below T_c it reduces to zero while pairing spreads to the antinodal region of the pseudogap leading to a *d*-wave superconducting gap on the entire Fermi surface at lower temperatures.

The properties of the pseudogap and its relation to the superconducting gap are among the central issues in the search for the cuprate pairing mechanism. A number of spectroscopic studies such as scanning tunneling microscopy (STM) and angle-resolved photoemission spectroscopy (ARPES) have been reported[1–14]. Some experiments indicate that the pseudogap may arise fully from precursor superconductivity (single-gap picture)[1–5], while others suggest an origin that is unrelated to superconductivity (two-gap picture)[6–14]. In the latter case, uncertainty exists as precursor pairing in certain temperature range above the superconducting transition temperature T_c is reported in some experiments[8,13,14], which contrast with other experiments in which the superconducting gap Δ_s is found to close at T_c[6,9,10,12]. In this paper, we address the issue using the temperature- and doping-dependent tunneling spectroscopy of submicron $Bi_2Sr_2CaCu_2O_{8+\delta}$ intrinsic Josephson junctions.

For conventional Bardeen-Cooper-Schrieffer (BCS) superconductors, Giaever's planar-type tunnel junctions[15] provided decisive measurements of the superconducting gap, the electronic density of states (DOS), the quasiparticle scattering rate, and the effective spectrum of phonons that mediate pairing[16–18]. $Bi_2Sr_2CaCu_2O_{8+\delta}$ intrinsic Josephson junctions[19] are the similar planar-type junctions with the best quality one may have for cuprate superconductors. As is shown in the inset of Fig. 1, these junctions are formed *within* the crystal with CuO_2 double-layers as superconducting electrodes and BiO/SrO interlayers as the tunnel barrier. Such superconductor-insulator-superconductor (SIS) junctions avoid all kinds of extrinsic uncertainties during experiment and can offer stable and reproducible temperature-dependent measurements. Earlier spectroscopic studies using these junctions suffered from sample's self-heating that severely distorts the tunneling spectra and many efforts were made to solve the problem[20–27]. One effort involved optimizing the surface-layer contact and reducing the junction size well below 1 μm, which are shown to suppress heating sufficiently in the case of near optimally doped samples[23–26]. The data presented below were based on these works and extended to samples with different doping strength.

The present work demonstrates that the superconducting gap Δ_s closes at a temperature T_{c0} well above T_c but far below the pseudogap opening temperature T^*, which supports a two-gap picture with superconducting pairing persisting up to T_{c0}. The pairing is found to occur first on a limited Fermi surface near the node below T_{c0}, accompanied by a Fermi arc due to finite quasiparticle scattering rate and pair decay rate. The arc length has a linear temperature dependence, and as temperature decreases below T_c it reduces to zero while pairing spreads to the antinodal region of the pseudogap leading to a *d*-wave superconducting gap on the entire Fermi surface at lower temperatures.

Results

Experimental spectra. In Fig. 1, we show the tunneling conductance $\sigma(V, T)$ at typical temperatures for four samples from underdoped (UD) to overdoped (OD) with $T_c = 71, 80, 89$ and 79 K, respectively (see Methods and

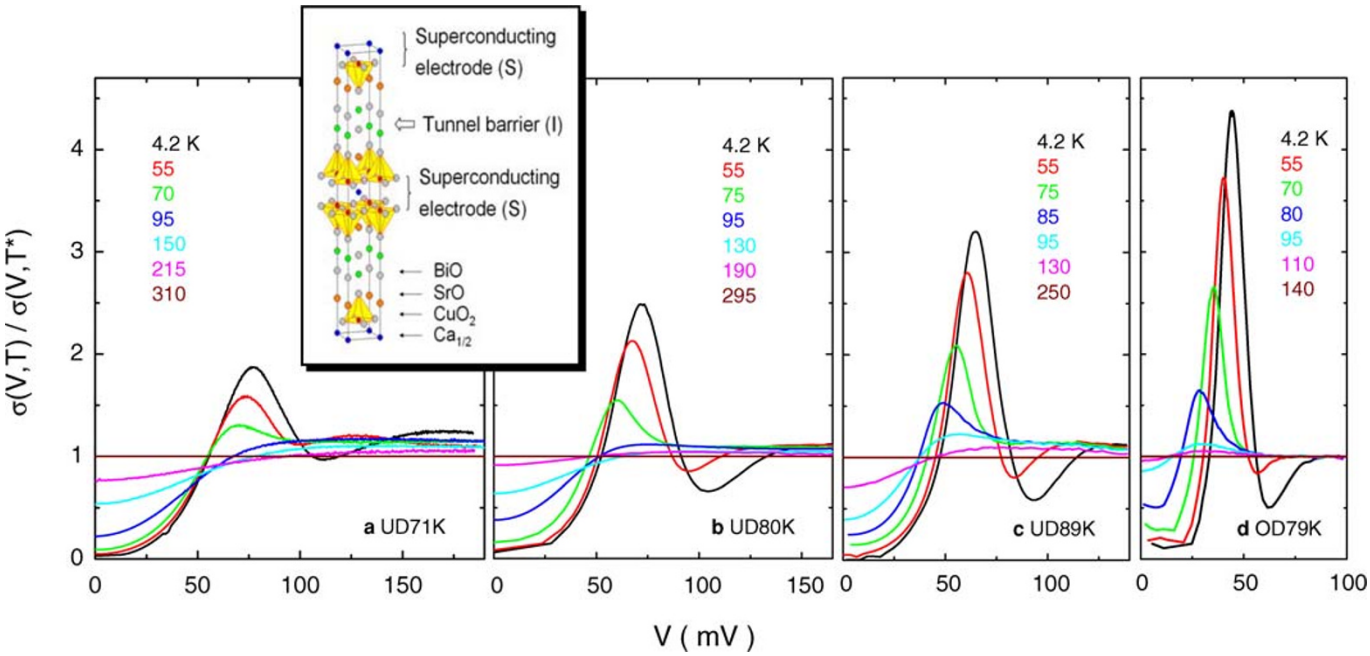

Figure 1 | Temperature and doping dependence of intrinsic tunneling spectra of $Bi_2Sr_2CaCu_2O_{8+\delta}$ superconductors. (a–d) doping strength increasing from underdoped (UD) to overdoped (OD) with T_c = 71, 80, 89 and 79 K, respectively. The spectra are presented with V corresponding to the voltage per junction and in each case are normalized to the respective ones at the pseudogap opening temperature T^* = 310, 280, 230 and 140 K. Inset displays a crystal unit cell, showing that electron tunneling occurs between CuO_2 double layers, which form planar-type superconductor-insulator-superconductor (SIS) tunnel junctions.

Supplementary Information for details). The data are normalized to $\sigma(V, T^*)$ with T^* = 310, 280, 230 and 140 K, above which the spectra become gapless. At low temperatures they exhibit the familiar peak-dip-hump structure with the superconducting coherence peak height and position, the peak-dip separation all evolving systematically with the doping strength. The dip feature, caused possibly by electron coupling to a Boson spectrum with energy linked to the peak-dip separation[28], disappears gradually as temperature approaches T_c.

In Fig. 2 a-d, we plot half the conductance peak position in meV versus temperature (squares), which represents Δ_s approximately at low temperatures. We see that for all samples the value decreases slightly with increasing temperature toward T_c, similar to the BCS gap versus temperature dependence. Near and above T_c, however, it differs substantially for different doping samples, which should result from the increasing roles played by the pseudogap and by the lifetime effects of the quasiparticles and Cooper pairs.

Temperature dependence of the superconducting gap. A key feature one expects for superconductors is that Δ_s follows the BCS-like gap equation and closes at a temperature, possibly higher than T_c[29], where Cooper pairs vanish. To clarify the situation, we fitted our experimental spectra with a DOS that is widely used in tunneling experiment for both BCS superconductors[18,30] and cuprates[1,26,31]:

$$N_s(\theta,\omega) = \mathrm{Re}\left[\frac{\omega + i\gamma_s}{\sqrt{(\omega+i\gamma_s)^2 - \Delta_s^2\cos^2(2\theta)}}\right]$$

where a d-wave gap is considered and the subscript s denotes the superconducting part. θ and γ_s are the angle of in-plane momentum measured from (π,0) (see Fig. 2e) and the parameter characterizing the lifetime effects, respectively. The DOS was first proposed by Dynes *et al.*[30] and recently shown[26] to be related to a phenomenological self-energy developed for the pseudogap discussion in which Δ_s extends to the precursor pairing regime above T_c[32]. Taking the UD89K data as an example, we replot half the peak position below T_c in Fig. 2f, in which lines are the BCS d-wave gap that closes at T^* (dashed), T_c (dotted) and T_{c0} = 140 K to be discussed below (solid). In the single-gap picture with pairing starting at T^*, Δ_s should vary along the dashed line near and above T_c if the lifetime effects are taken into account. Δ_s obtained from fit to the normalized spectra $\sigma(V, T)/\sigma(V, T^*)$ using $N_s(\theta, \omega)$ over the whole Fermi surface[26] is shown in Fig. 2f as open squares (γ_s not shown for clarity). It is seen that the result deviates significantly from the dashed line, which means that the single-gap picture does not lead to an appropriate description.

In an STM experiment on $Bi_2Sr_2CuO_{6+\delta}$ superconductors, Boyer *et al.*[6] found that when seemingly irregular experimental spectra are normalized to the one slightly above T_c, they reveal a homogeneous superconducting gap that closes at T_c. This treatment eliminates the effect of the pseudogap that already exists above T_c. (Such treatment was also applied for $Bi_2Sr_2CaCu_2O_{8+\delta}$ SIS-type junctions[28] and BCS SIS-type junctions where effects unrelated to superconductivity are successfully removed[16]). In the related two-gap picture, one may view the two phases as coexisting and being anticorrelated on the Fermi surface with different spectral weights, and there is a boundary θ_p below and above which they dominate respectively[11]. Fig. 2e shows a simple cut-off presentation as used in STM experiments[7,8]. In the present work, we fitted the normalized spectra $\sigma(V, T)/\sigma(V, T_c)$, considering consistently $N_s(\theta, \omega)$ for $\theta > \theta_p$ only on the Fermi surface so the pseudogap-dominant region was excluded in the tunneling current calculation (see Methods). The resulting Δ_s taking θ_p = 12°, a value close to the STM observation[7], is shown as open circles in Fig. 2f for the UD89K sample. It can be seen that the fit is again unsatisfactory when compared to the BCS curve (dotted line).

A satisfactory fit was nevertheless obtained when it was performed with respect to $\sigma(V, T)/\sigma(V, T_{c0})$ where $T_c < T_{c0} < T^*$, for which pair formation starting at T_{c0} should be assumed. Precursor pairing above T_c has been suggested previously in some experiments[8,13,14,33,34]. We note that the half peak position in Fig. 2c (squares) shows an obvious turning near 140 K. In Fig. 2f (also in c), Δ_s from the fit considering T_{c0} = 140 K and excluding the pseudogap region of $\theta < \theta_p$ = 12° is shown as solid up-triangles. We see that Δ_s follows nicely the BCS

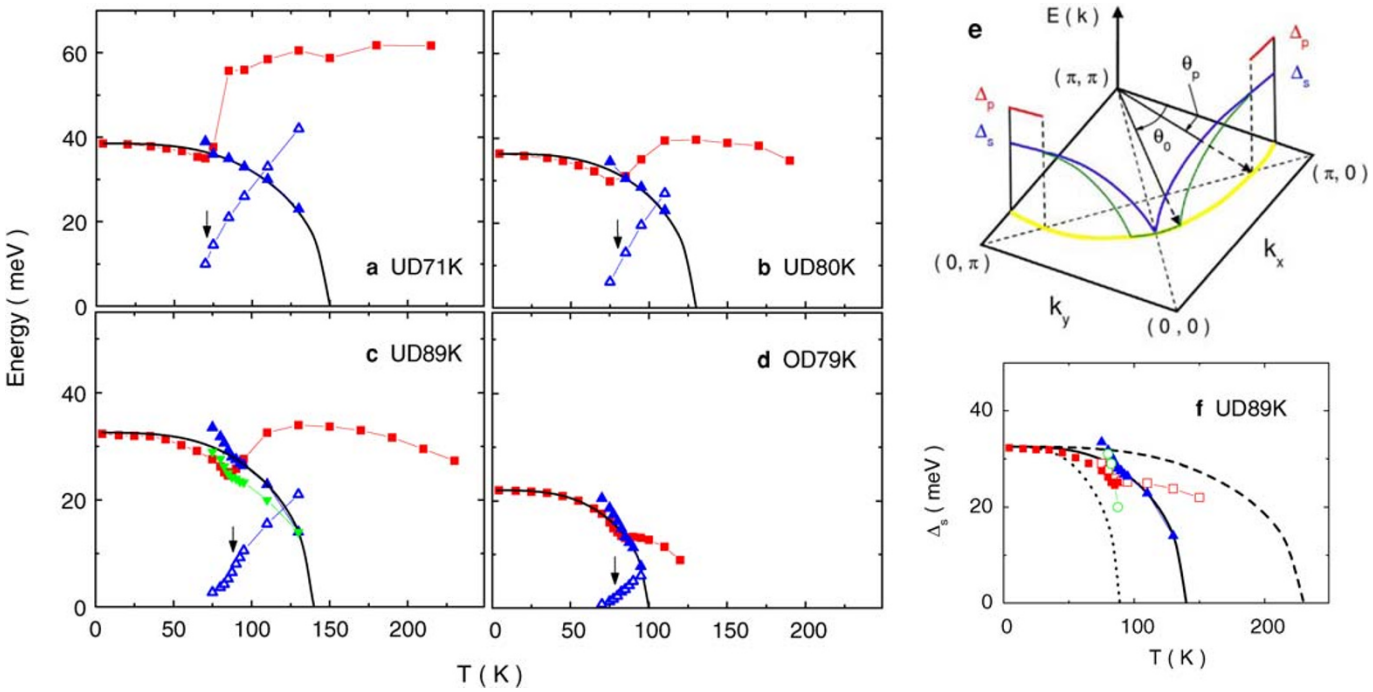

Figure 2 | Measured and fitted quantities showing that the superconducting gap Δ_s closes at T_{c0} ($T_c < T_{c0} < T^*$), above which a pseudogap already exists. (a–d) squares: half the conductance peak position in meV; up-triangles: superconducting gap Δ_s (solid) and lifetime parameter γ_s (open) obtained by fitting the normalized spectra $\sigma(V, T)/\sigma(V, T_{c0})$ using $N_s(\theta, \omega)$ excluding the pseudogap-dominant region from 0 to θ_p on the Fermi surface. Above T_c (indicated by arrows), Δ_s is seen to follow nicely the BCS *d*-wave gap (lines) closing at T_{c0} = 150, 130, 140, 100 K, respectively. In (c) Δ_s obtained from fit considering the entire Fermi surface is plotted as down-triangles for comparison. (e) symbols and schematic gap profiles on the Fermi surface (yellow) in the temperature ranges of well below T_c (blue) and from T_{c0} to T^* (red). From near T_c to T_{c0}, half the peak separation of $A(k_F, \omega)$ is shown (green) with a Fermi arc as observed in ARPES experiment. (f) Δ_s of the UD89K sample obtained from fits to the normalized $\sigma(V, T)/\sigma(V, T^*)$ (open squares) and $\sigma(V, T)/\sigma(V, T_c)$ (circles) tunneling spectra. Both deviate considerably from the BCS gap closing at respective temperatures (dashed and dotted lines), as compared to the result from fit to $\sigma(V, T)/\sigma(V, T_{c0})$ (up-triangles, also in c) that shows a good agreement with the BCS prediction (solid line) above T_c (see text for more details).

curve (solid line) above T_c in this case. As temperature decreases below T_c, however, it deviates increasingly with decreasing temperature. To understand this behavior, we also plot Δ_s obtained with $\theta_p = 0$ as down-triangles in Fig. 2c, which shows a clear tendency of approaching the BCS solid line below T_c. These two results can be naturally explained if, as temperature decreases below T_c, the superconducting pairing gradually spreads to the antinode on the Fermi surface with $\theta < \theta_p$, which is predominantly occupied by the pseudogap phase above T_c.

Similar results were obtained for other samples and they are displayed in Fig. 2a-d together with the fitted γ_s shown as open up-triangles. T_{c0} from the best fit for the four samples is 150, 130, 140 and 100 K, respectively. For the more underdoped UD71K sample, pair spreading into the antinodal region is seen in a more limited temperature range below T_c since a tunneling dip quickly develops, which is beyond the simple description using $N_s(\theta, \omega)$[28]. On the other hand, all the data above T_c show a compelling evidence that the superconducting gap Δ_s closes at T_{c0}. They demonstrate that the superconducting phase grows out from the pseudogap phase with T_{c0} as the Cooper pair formation temperature, which supports a two-gap picture with precursor pairing extending from above T_c up to T_{c0}.

Temperature dependence of the zero-bias conductance. Additional evidence that the superconducting gap Δ_s closes (or opens if we look with decreasing temperature) at T_{c0} came from the direct experimental data of the zero-bias conductance $\sigma(0, T)$, which should be largely related to the density of states near the Fermi level and thus is sensitive to the formation of an energy gap. In Fig. 3, we plot the measured $\sigma(0, T)/\sigma(0, T^*)$ for the four samples in the temperature range from 4.2 K to T^*. The up and down arrows indicate T_{c0} and T_c, respectively. It can be seen that with lowering temperature an accelerated decrease occurs starting from T_{c0} for all samples, which corresponds to the fast decrease of the density of states resulting from the opening of the superconducting gap Δ_s. Also, such a decrease is seen to continue farther below T_c for higher doping samples. This can be explained considering that for higher doping samples, T_c is closer to T_{c0} so Δ_s will increase more below T_c before reaching the low-temperature value (see Fig. 2), which leads to the further reduction of $\sigma(0, T)$.

Parameters of the superconducting and pseudogap phases. We emphasize that our fit based on $\sigma(V, T)/\sigma(V, T_{c0})$ assumes a temperature-independent pseudogap. As is discussed by Boyer *et al.*[6] this should be a reasonable approximation. In many experiments such as STM[1] the pseudogap peak position is found nearly temperature independent and it disappears by "filling-up" as temperature approaches T^*. If we take the half peak position at T_{c0} in Fig. 2 a-d to characterize the pseudogap Δ_p, it shows a distinct doping dependence as that of Δ_s. In Fig. 4a, we plot T^*, T_{c0} and T_c against the doping level p, while Δ_s and Δ_p are shown in Fig. 4b and the resulting $2\Delta_s/kT_{c0}$ in the inset. In Fig. 4b, Δ_p is seen to have a fast increase as p reduces to the more underdoped level, as observed in ARPES experiments[35]. On the overdoped side, it continues to decrease to a value below Δ_s.

Fermi arcs derived from lifetime parameters. The lifetime effects play an important role in the precursor pairing regime from around T_c up to T_{c0} due to increasing γ_s. One of the consequences is the appearance of a Fermi arc near the node with $\theta > \theta_0$ (see Fig. 2e), which is defined through the peak separation of the spectral function

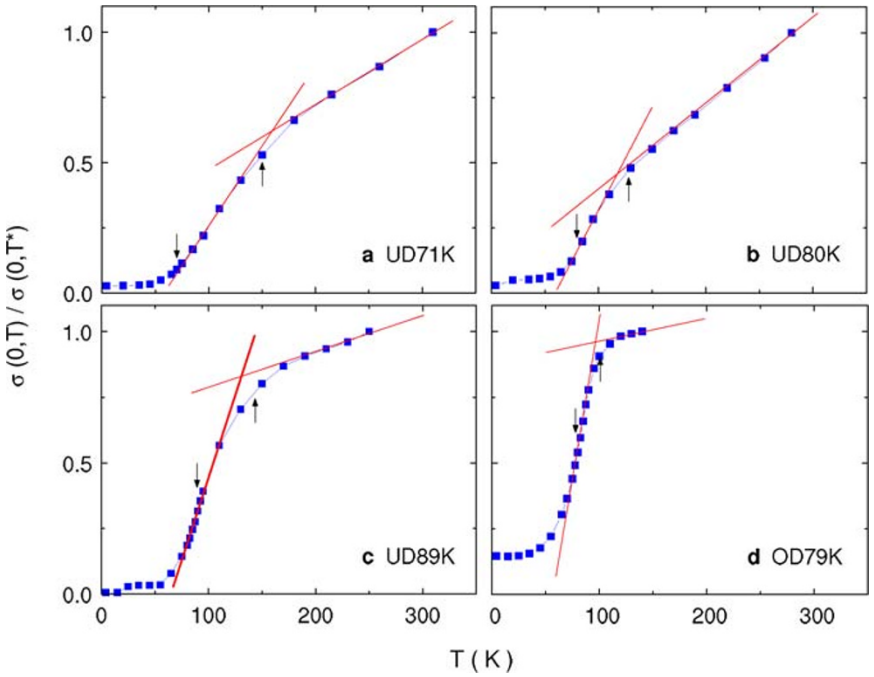

Figure 3 | Temperature dependence of the zero-bias conductance. The data are presented from 4.2 K up to the pseudogap opening temperature T^* and are normalized to those at T^*. Arrows pointing upward and downward indicate T_{c0} and T_c, respectively. Solid lines are guides to the eye.

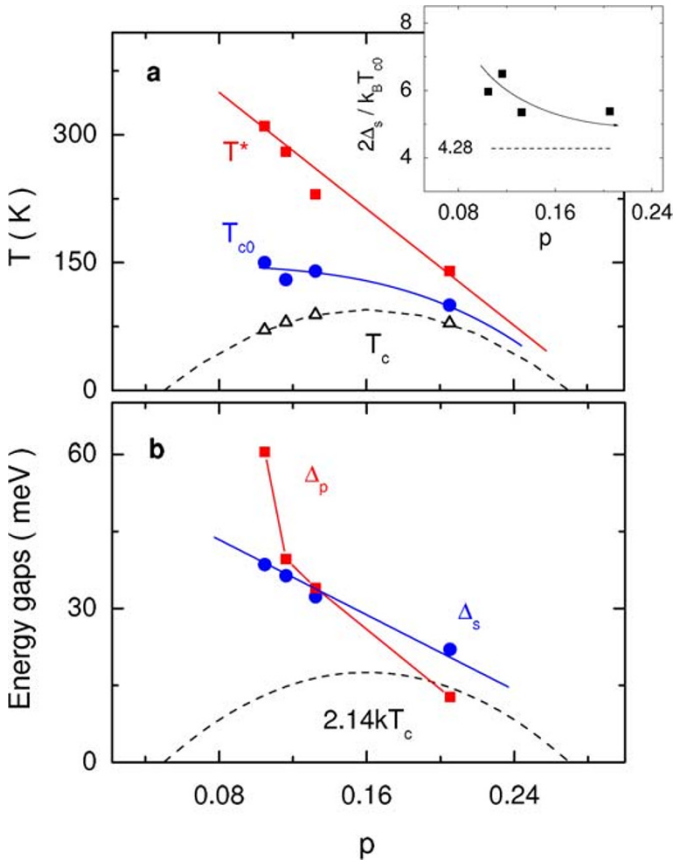

Figure 4 | Doping dependence of superconducting and pseudogap phases parameters. (a) T_c, T_{c0} and T^*. (b) Δ_s and Δ_p. Inset shows $2\Delta_s/k_BT_{c0}$. Hole concentration p is obtained from the relation $T_c/T_{c,max} = 1–82.6(p - 0.16)^2$ with $T_{c,max} = 95$ K. Solid lines are guides to the eye.

$A(\mathbf{k}, \omega)$ around Fermi surface in ARPES experiments[36,37]. The above-mentioned self-energy model[32], from which $N_s(\theta, \omega)$ can be derived[26], contains three parameters: the quasiparticle scattering rate Γ, the pair decay rate Γ_Δ, and Δ_s, with $\gamma_s = (\Gamma + \Gamma_\Delta)/2$. Assuming a linear temperature dependence of Γ, we inferred both Γ and Γ_Δ from the fitted parameters γ_s in Fig. 2a-d. With known Δ_s, Γ and Γ_Δ, $A(k_F, \omega)$ was determined and the arc length $l_{arc} = 1 - (4/\pi)\theta_0$ was calculated[26,36,37] (see Methods). In Fig. 5, we show the calculated l_{arc} versus temperature for the four samples. The results display an approximate linear temperature dependence, which is quite general as discussed in the ARPES data analysis using the same self-energy in a simplified situation of $\Gamma = \Gamma_\Delta$[36,37].

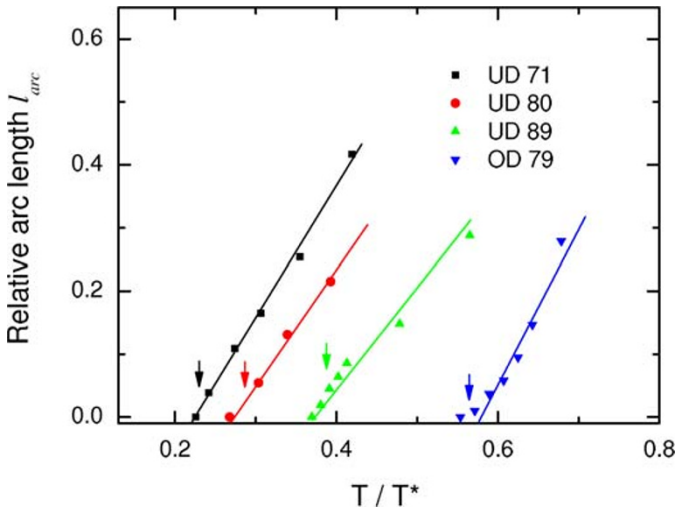

Figure 5 | Temperature dependence of relative arc length l_{arc} calculated from fitted Δ_s, Γ and Γ_Δ parameters. Arrows indicate T_c. Solid lines are guides to the eye showing approximately the linear temperature dependence.

Discussion

We have shown that for the four $Bi_2Sr_2CaCu_2O_{8+\delta}$ crystals with different doping levels the superconducting gap Δ_s closes at a temperature T_{c0} well above the superconducting transition temperature T_c but far below the pseudogap opening temperature T^* thus an extensive precursor pairing regime between T_c and T_{c0} is demonstrated. In the Methods section, we present an alternative fitting procedure considering both the superconducting part (Δ_s, γ_s) and the pseudogap part (Δ_p, γ_p), which leads to the same conclusion as using the conventional approach of normalizing out the pseudogap contribution described above. It is shown that Δ_p is nearly constant from slightly below T_c up to T^* while γ_p experiences a continuous increase, which is consistent with the filling-up character of the pseudogap as temperature approaches T^* from below.

So far the STM and ARPES results supporting the two-gap scenario alone for the $Bi_2Sr_2CaCu_2O_{8+\delta}$ materials are still diverse and controversial. Some results suggest that below T_c the superconducting gap would coexist with the pseudogap at the antinode[12,13] while others indicate that they reside at the nodal and antinodal regions separately[7]. Above T_c, precursor pairing is demonstrated in some experiments[8,13] whereas a superconducting gap closing at T_c is also observed[9]. The present tunneling results clearly support the precursor pairing view in the temperature range from T_c to T_{c0}, which is similar to the results in Refs. 8 and 13. In this temperature range, the superconducting gap and the pseudogap locate predominantly at the node and the antinode, respectively. We note that both the results of Δ_s presented as solid up- and down-triangles in Fig. 2c are obtained by fitting to the spectra that are normalized to the one at T_{c0}. In this case, the pseudogap contribution is not considered in the fits but it still exists. Therefore the result that the superconducting pairing spreads into the antinodal region below T_c means that the two components coexist at the antinode. Since all the data of Δ_s in Fig. 2a–d (solid up-triangles) show similar upturns as temperature decreases below T_c, we believe the coexisting nature to be true for all samples. On the other hand, for the UD71K sample we see from Fig. 2a (squares) that the pseudogap spectral peak quickly diminishes and switches to the superconducting peak below T_c. This may indicate that the spectral weight of the pseudogap becomes small compared to that of the superconducting gap below T_c for this sample which is still not deep enough into underdoping, or the pseudogap structure is obscured by the growth of the dip structure in the tunneling spectra. For higher doping samples, uncertainty arises from the fact that the superconducting gap and pseudogap scales becomes similar (see Fig. 2).

Fermi arcs in the ARPES experiments often show a relatively large size just above T_c, which collapse as temperature decreases below T_c[3,9,38]. In the two-gap scenario, the collapse results from the opening of the superconducting gap on the arc at T_c[9]. Our results are similar to those in a sense that T_{c0} is in the place of T_c and the arc region is defined from θ_p to $\pi/2$ - θ_p in Fig. 2e in the pseudogap state. As mentioned above, the lifetime effects in the superconducting state can be successfully used to explain the linear temperature dependence of the arc length l_{arc}[36,37]. It is interesting to note that in the single-gap picture l_{arc} will exhibit a faster rise as temperature increases across T_c and therefore has a larger value compared to those in Fig. 5 just above T_c[26], which is consistent with the results observed in ARPES experiments[3,38]. On the other hand, our present results, including the development of the superconducting gap at $T_{c0} > T_c$ on an arc spanned in the pseudogap state and the temperature dependence of the arc resulting from the lifetime effects in the superconducting state, as depicted in Fig. 5, bear a close resemblance to the STM observations[8,29]. The differences and similarities in these ARPES and tunneling experiments remain to be explained in the future.

Open questions that are of further interest are the nature of the pseudogap and whether the superconducting and pseudogap phases are formed from the same underlying physics. Recent experiments suggest that the pseudogap phase can result from various density-wave and other states, which may compete[11] or have an intimate relationship with the superconducting state[14]. Our results indicate that the pseudogap Δ_p has a distinct temperature and doping dependence compared to Δ_s, which may not be in favor of the view that they have a common microscopic origin. In the classical BCS superconductors, the strong Coulomb and phonon interactions between electrons in the normal state lead to an average correlation energy in the order of eV, which is much larger than the pair-binding energy of meV. The strong interactions are later removed in Landau's Fermi-liquid theory with quasiparticles replacing the bare electrons. Consideration of the interaction neglected in Landau's approximation leads to the coupling between quasiparticles and formation of Cooper pairs[17]. In the present case of cuprate superconductors, however, the situation is different and is more complicated as we see that the pseudogap size can be larger, comparable, and smaller than the superconducting gap when doping increases.

Methods

Experimental details. Mesa-type intrinsic Josephson junctions (IJJs)[19–27] were used in this work with their geometry shown schematically in Fig. S1. Details of the sample fabrication have been described elsewhere[23,24]. To reduce samples self-heating, a notorious problem in IJJs studies, we took special care to reduce the contact resistance between Au films and $Bi_2Sr_2CaCu_2O_{8+\delta}$ crystals which results in the surface layers with good properties[23,25]. In addition, mesa sizes were reduced well below 1 μm as it was demonstrated that heating can be largely neglected in this case[24]. Other methods to reduce heating include using IJJs made of $HgBr_2$ intercalated $Bi_2Sr_2CaCu_2O_{8+\delta}$ crystals[20,27] and adopting short-pulse measurements[21], which are discussed extensively recently[27]. These studies demonstrate tunneling spectra with moderate sharpness of the conductance peak and clear presence of the dip feature after the reduction of heating, as achieved in the present experiment shown in Fig. 1. (See Supplementary Information for further details.)

Spectra fit separating the pseudogap contribution. The *I-V* characteristics of a superconductor-insulator-superconductor (SIS) junction can be calculated from[18]:

$$I(V) = \frac{1}{eR_N}\int_{-\infty}^{\infty} n(\omega)n(\omega+eV)[f(\omega)-f(\omega+eV)]d\omega \qquad (1)$$

where R_N is junction's normal-state resistance, $n(\omega)$ is the DOS of two identical S-electrodes and $f(\omega)$ is the Fermi function. Our results were obtained by fitting the normalized experimental spectra using $\sigma = dI/dV$ from equation (1) with the following normalized DOS for $n(\omega)$:

$$N_{eff}(\omega) = \frac{1}{C}\int_{\theta_p}^{\pi/4} N_s(\theta,\omega)\cos^2(2\theta)d\theta, \quad C = \frac{\pi}{8} - \frac{\theta_p}{2} - \frac{\sin 4\theta_p}{8}, \qquad (2)$$

where $\cos^2(2\theta)$ comes from the directional tunneling matrix element, which is found to improve the description for the intrinsic tunneling process within $Bi_2Sr_2CaCu_2O_{8+\delta}$ crystals[26–28]. In equation (2), integration is performed from θ_p to $\pi/4$ with $\theta_p \geq 0$ due to symmetry. If the superconducting phase is considered on the entire Fermi surface, we have $\theta_p = 0$. As discussed in the paper, our central results in Fig. 2a–d were obtained from fitting $\sigma(V,T)/\sigma(V, T_{c0})$ with a nonzero θ_p to exclude the pseudogap-dominant region on the Fermi surface.

The θ_p parameters obtained from fits to the four samples used in this work are listed in Table SI. For samples from UD89K to OD79K, θ_p decreases from 12° to 10°. This trend is consistent with the STM observations[7]. However, for UD80K and UD71K samples, θ_p is 10° and 11°. The slight inconsistency could be caused by the fact that the UD80K and UD71K samples were yttrium doped, which were different from the oxygen doped UD89K and OD79K samples and might have altered crystalline arrangement resulting in reduced pseudogap expansion in momentum space. The satisfactoriness of our fit using these parameters can be seen in Fig. S4.

Using normalized spectra to get rid of the effects unrelated to superconductivity is a common practice in tunneling experiments for both BCS superconductors[16,18] and cuprates[6,28] in both SIN (N being a normal metal)[6,18] and SIS[16,28] type tunnel junctions. For example, McMillan and Rowell studied the SIS type Pb junctions[16]. By normalizing the data below T_c to the one above T_c, additional structures in the measured spectra resulting from tunnel barrier phonons are successfully removed. The phonon spectra extracted from the data are exactly the same as those obtained from the SIN type Pb junctions. Below we further justify this approach for the present experiment by considering both the superconducting and pseudogap contributions in the fitting procedure.

According to the two-gap scenario, from T_{c0} up to T^* there is only the pseudogap phase located predominantly near the antinode with $\theta < \theta_p$ and one has $N_s(\theta, \omega) = 1$ for $\theta > \theta_p$. Below T_{c0} down to at least T_c the superconducting and pseudogap phases

exist predominantly above and below θ_p, respectively (see Fig. 2e). If we use the same form of *d*-wave DOS to model the pseudogap phase that may come from various density-wave states, now denoted by $N_p(\theta, \omega)$ with two parameters Δ_p and γ_p, we can write the following DOS for $n(\omega)$ in equation (1) for $T > T_{c0}$:

$$N_>(\omega) = \frac{8}{\pi}\int_0^{\theta_p} N_p(\theta,\omega)\cos^2(2\theta)d\theta + \frac{8}{\pi}\int_{\theta_p}^{\pi/4}\cos^2(2\theta)d\theta \equiv D_p(\omega) + C_s, \quad (3)$$

where C_S is a constant from the ungapped part on the Fermi surface. For $T < T_{c0}$ we have

$$N_<(\omega) = D_p(\omega) + \frac{8}{\pi}\int_{\theta_p}^{\pi/4} N_s(\theta,\omega)\cos^2(2\theta)d\theta \equiv D_p(\omega) + D_s(\omega). \quad (4)$$

The *I-V* curve can be calculated above T_{c0} from

$$I_>(V) = \frac{1}{eR_N}\int_{-\infty}^{\infty}\left[D_p(\omega)+C_s\right]\left[D_p(\omega+eV)+C_s\right][f(\omega)-f(\omega+eV)]d\omega, \quad (5)$$

and below T_{c0} from

$$I_<(V) = \frac{1}{eR_N}\int_{-\infty}^{\infty}\left[D_p(\omega)+D_s(\omega)\right]\left[D_p(\omega+eV)+D_s(\omega+eV)\right][f(\omega)-f(\omega+eV)]d\omega. \quad (6)$$

In Fig. S5, we show the results from fits using $I_>(V)$ and $I_<(V)$ to the normalized experimental spectra $\sigma(V, T)/\sigma(V, T^*)$ (note that T* is used as normalization temperature instead of T_{c0}), taking also the UD89K IJJs as the example. Up-triangles are replotted Δ_s and γ_s from Fig. 2c and 2f. Above T_{c0}, only the pseudogap is concerned, the parameters Δ_p and γ_p are thus directly determined using $I_>(V)$, which are shown as down-triangles above T_{c0}. The down-triangles shown in the figure below T_{c0} are obtained using $I_<(V)$ and the replotted Δ_s and γ_s parameters. In other words, if these Δ_p and γ_p are used, the two fitting approaches would produce the same Δ_s and γ_s. For comparison, squares in Fig. S5 show the Δ_s and γ_s when Δ_p and γ_p values at 150 K are used for temperatures below T_{c0}. These data show nearly the same Δ_s but slightly different γ_s.

These results confirm our central conclusion that the superconducting gap Δ_s closes at T_{c0}. We note that Δ_p in Fig. S5 is nearly constant while γ_p increases with increasing temperature all the way up to T^*, which demonstrate that the pseudogap disappears by "filling-up" as temperature approaches T^*. Since a continuing decrease of γ_p down to T_c seems reasonable, both Δ_s and γ_s parameters obtained from the simple fitting approach using $\sigma(V, T)/\sigma(V, T_{c0})$ and equations (1) and (2) should be a good approximation.

Fermi arc calculation. For the discussion of the cuprate pseudogap in ARPES experiments, Norman *et al.* proposed a phenomenological self-energy taking account of the lifetime effects[32]:

$$\sum(\mathbf{k},\omega) = -i\Gamma + \frac{\Delta_{\mathbf{k}}^2}{\omega + \epsilon_{\mathbf{k}} + i\Gamma_\Delta}, \quad (7)$$

where $\epsilon_{\mathbf{k}}$ is the energy of bare electrons relative to the value at the Fermi surface. From equation (7) it can be shown that the Green's function $G(\mathbf{k}, \omega) = 1/[\omega - \epsilon_{\mathbf{k}} - \Sigma(\mathbf{k}, \omega)]$ has the form

$$G(\mathbf{k},\omega) = \frac{\omega + i\Gamma_\Delta + \epsilon_{\mathbf{k}}}{(\omega + i\Gamma - \epsilon_{\mathbf{k}})(\omega + i\Gamma_\Delta + \epsilon_{\mathbf{k}}) - \Delta_{\mathbf{k}}^2}. \quad (8)$$

The spectral function on the Fermi surface $A(k_F, \omega) = -(1/\pi)\mathrm{Im}G(k_F, \omega)$, assuming $\Delta_k = \Delta_s \cos(2\theta)$, is given by[26]

$$A(\theta,\omega) = \frac{1}{\pi}\frac{\Gamma_\Delta\left[\Delta_s^2\cos^2(2\theta) + \Gamma\Gamma_\Delta\right] + \Gamma\omega^2}{\left[\omega^2 - \Delta_s^2\cos^2(2\theta) - \Gamma\Gamma_\Delta\right]^2 + \omega^2(\Gamma + \Gamma_\Delta)^2}. \quad (9)$$

In the ARPES experiments, it is considered to be gapped if $A(k_F, \omega)$ has maxima at $\omega = \pm\omega_p \neq 0$, while Fermi arc appears at places where $A(k_F, \omega)$ has maximum only at $\omega = 0$. Thus ω_p can be found by setting the first derivative of equation (9) to zero:

$$\omega_p^2 = \left(1 + \frac{\Gamma_\Delta}{\Gamma}\right)\Delta_s\cos(2\theta)\sqrt{\eta} - \frac{\Gamma_\Delta}{\Gamma}\eta, \quad (10)$$

where $\eta = \Delta_s^2\cos^2(2\theta) + \Gamma\Gamma_\Delta$. By setting the second derivative to zero, the angle θ_0 at which the arc starts is found to be

$$\theta_0 = 0.5\cos^{-1}\left(\sqrt{\frac{\Gamma_\Delta}{\Gamma + 2\Gamma_\Delta}}\frac{\Gamma_\Delta}{\Delta_s}\right). \quad (11)$$

The relative arc length l_{arc} is defined by

$$l_{arc} = 1 - \left(\frac{4}{\pi}\right)\theta_0. \quad (12)$$

In the present work, the quasiparticle scattering rate Γ and pair decay rate Γ_Δ were estimated from the experimentally fitted parameter γ_s in Fig. 2a–d via the relation $\gamma_s = (\Gamma + \Gamma_\Delta)/2$[26]. We assumed a linear temperature dependence of Γ and considered that Γ is larger than Γ_Δ, which should be reasonable from the basic physical considerations. In Fig. S6 the results of Γ and Γ_Δ for the four samples are shown, which were determined considering that $\Gamma_\Delta = 0$ near T_c and the slope of Γ set close to that of γ_s. The corresponding l_{arc} versus T calculated are plotted in Fig. 5.

1. Fischer, ϕ., Kugler, M., Maggio-Aprile, I., Berthod, C. & Renner, C. Scanning tunneling spectroscopy of high-temperature superconductors. *Rev. Mod. Phys.* **79**, 353–419 (2007).
2. Shi, M. *et al.* Coherent d-wave superconducting gap in underdoped $La_{2-x}Sr_xCuO_4$ by Angle-Resolved Photoemission Spectroscopy *Phys. Rev. Lett.* **101**, 047002 (2008).
3. Nakayama, K. *et al.* Evolution of a pairing-induced pseudogap from the superconducting state gap of $(Bi,Pb)_2Sr_2CuO_6$. *Phys. Rev. Lett.* **102**, 227006 (2009).
4. Meng, J. *et al.* Monotonic d-wave superconducting gap of the optimally doped $Bi_2Sr_{1.6}La_{0.4}CuO_6$ superconductor by laser-based angle-resolved photoemission spectroscopy. *Phys. Rev. B* **79**, 024514 (2009).
5. Chatterjee, U. *et al.* Observation of a *d*-wave nodal liquid in highly underdoped $Bi_2Sr_2CaCu_2O_{8+\delta}$. *Nat. Phys.* **6**, 99–103 (2010).
6. Boyer, M. C. *et al.* Imaging the two gaps of the high-temperature superconductor $Bi_2Sr_2CuO_{6+\delta}$. *Nat. Phys.* **3**, 802–806 (2007).
7. Kohsaka, Y. *et al.* How Cooper pairs vanish approaching the Mott insulator in $Bi_2Sr_2CaCu_2O_{8+\delta}$. *Nature* **454**, 1072–1078 (2008).
8. Lee, J. *et al.* Spectroscopic fingerprint of phase-incoherent superconductivity in the underdoped $Bi_2Sr_2CaCu_2O_{8+\delta}$. *Science* **325**, 1099–1103 (2009).
9. Lee, W. S. *et al.* Abrupt onset of a second energy gap at the superconducting transition of underdoped Bi2212. *Nature* **450**, 81–84 (2007).
10. Ma, J.-H. *et al.* Coexistence of competing orders with two energy gaps in real and momentum space in the high temperature superconductor $Bi_2Sr_{2-x}La_xCuO_{6+\delta}$. *Phys. Rev. Lett.* **101**, 207002 (2008).
11. Kondo, T. *et al.* Competition between the pseudogap and superconductivity in the high-Tc copper oxides. *Nature* **457**, 296–300 (2009).
12. Vishik, I. M. *et al.* ARPES studies of cuprate Fermiology: superconductivity, pseudogap and quasiparticle dynamics. *New J. Phys.* **12**, 105008 (2010).
13. Kondo, T. *et al.* Disentangling Cooper-pair formation above the transition temperature from the pseudogap state in the cuprates. *Nat. Phys.* **7**, 21–25 (2011).
14. He, Rui-Hua *et al.* From a single-band metal to a high-temperature superconductor via two thermal phase transitions. *Science* **331**, 1579–1583 (2011).
15. Giaever, I. Energy gap in superconductors measured by electron tunneling. *Phys. Rev. Lett.* **5**, 147 (1960).
16. McMillan, W. L. & Rowell, J. M. Tunneling and strong-coupling superconductivity, in *Superconductivity*, edited by R. D. Parks (Marcel Dekker, New York, 1969).
17. Schrieffer, J. R. *Theory of Superconductivity*, (Benjamin, New York, 1964).
18. Wolf, E. L. *Principles of Electron Tunneling Spectroscopy*, (Oxford University Press, New York, 1985).
19. Kleiner, R. *et al.* Intrinsic Josephson effects in $Bi_2Sr_2CaCu_2O_8$ single crystals. *Phys. Rev. Lett.* **68**, 2394 (1992).
20. Yurgens, A. *et al.* Pseudo-gap features of intrinsic tunneling in $(HgBr_2)$-Bi2212 single crystals. *Int. J. Mod. Phys. B* **13**, 3758–3763 (1999).
21. Anagawa, K. *et al.* 60 ns time scale short pulse interlayer tunneling spectroscopy for $Bi_2Sr_2CaCu_2O_{8+\delta}$. *Appl. Phys. Lett.* **83**, 2381–2383 (2003).
22. Krasnov, V. M., Sandberg, M. & Zogaj, I. In situ measurement of self-heating in intrinsic tunneling spectroscopy. *Phys. Rev. Lett.* **94**, 077003 (2005).
23. Zhao, S. P. *et al.* $Bi_2Sr_2CaCu_2O_{8+\delta}$ intrinsic Josephson junctions: Surface layer characterization and control. *Phys. Rev. B* **72**, 184511 (2005).
24. Zhu, X. B. *et al.* Intrinsic tunneling spectroscopy of $Bi_2Sr_2CaCu_2O_{8+\delta}$: The junctionsize dependence of self-heating. *Phys. Rev. B* **73**, 224501 (2006).
25. Li, S. X. *et al.* Observation of macroscopic quantum tunneling in a single $Bi_2Sr_2CaCu_2O_{8+\delta}$ surface intrinsic Josephson junction. *Phys. Rev. Lett.* **99**, 037002 (2007).
26. Zhao, S. P., Zhu, X. B. & Tang, H. Tunneling spectra of submicron $Bi_2Sr_2CaCu_2O_{8+\delta}$ intrinsic Josephson junctions: evolution from superconducting gap to pseudogap. *Eur. Phys. J. B* **71**, 195–201 (2009).
27. Kurter, C. *et al.* Counterintuitive consequence of heating in strongly-driven intrinsic junctions of $Bi_2Sr_2CaCu_2O_{8+\delta}$ mesas. *Phys. Rev. B* **81**, 224518 (2010).
28. Zasadzinski, J. F. *et al.* Persistence of strong electron coupling to a narrow boson spectrum in overdoped $Bi_2Sr_2CaCu_2O_{8+\delta}$ tunneling data. *Phys. Rev. Lett.* **96**, 017004 (2006).
29. Pasupathy, A. N. *et al.* Electronic origin of the inhomogeneous pairing interaction in the high-T_c superconductor $Bi_2Sr_2CaCu_2O_{8+\delta}$. *Science* **320**, 196–201 (2008).
30. Dynes, R. C., Narayanamurti, V. & Garno, J. P. Direct measurement of quasiparticlelifetime broadening in a strong-coupled superconductor. *Phys. Rev. Lett.* **41**, 1509 (1978).
31. Miyakawa, N. *et al.* Strong dependence of the superconducting gap on oxygen doping from tunneling measurements on $Bi_2Sr_2CaCu_2O_{8-\delta}$. *Phys. Rev. Lett.* **80**, 157 (1998).
32. Norman, M. R. *et al.* Phenomenology of the low-energy spectral function in high-T_c superconductors. *Phys. Rev. B* **57**, R11093 (1998).

33. Wang, Y. *et al.* Field-enhanced diamagnetism in the pseudogap state of the cuprate $Bi_2Sr_2CaCu_2O_{8+\delta}$ superconductor in an intense magnetic field. *Phys. Rev. Lett.* **95**, 247002 (2005).
34. Wen, H. H. *et al.* Specific-heat measurement of a residual superconducting state in the normal state of underdoped $Bi_2Sr_{2-x}La_xCuO_{6+\delta}$ cuprate superconductors. *Phys. Rev. Lett.* **103**, 067002 (2009).
35. Ideta, S. *et al.* Enhanced superconducting gaps in the trilayer high-temperature $Bi_2Sr_2Ca_2Cu_3O_{10+\delta}$ cuprate superconductor. *Phys. Rev. Lett.* **104**, 227001 (2010).
36. Norman, M. R. *et al.* Modeling the Fermi arc in underdoped cuprates. *Phys. Rev. B* **76**, 174501 (2007).
37. Chubukov, A. V. *et al.* Gapless pairing and the Fermi arc in the cuprates. *Phys. Rev. B* **76**, R180501 (2007).
38. Kanigel, A. *et al.* Protected nodes and the collapse of Fermi arcs in high-T_c cuprate superconductors. *Phys. Rev. Lett.* **99**, 157001 (2007).

Acknowledgements

We thank N. P. Ong, Siyuan Han, X. J. Zhou and Z. Y. Weng for helpful discussions. This work was supported by the National Natural Science Foundation of China (Grant Nos. 10974242 and 50825206) and the Ministry of Science and Technology of China (Grant No. 2011CBA00106).

Author contributions

J.K.R., X.B.Z., Y.F.R., H.F.Yang and C.Z.G. prepared the mesa samples. J.K.R., X.B.Z., H.F.Yu and Ye T. did the measurement. J.K.R. and S.P.Z. performed the data analysis. N.L.W. provided and prepared single crystals for the UD71K, UD80K and OD79K samples. S.P.Z. designed the experiment and wrote the manuscript.

Additional information

Supplementary information accompanies this paper at http://www.nature.com/scientificreports

Competing financial interests: The authors declare no competing financial interests.

How to cite this article: Ren, J.K. *et al.* Energy gaps in $Bi_2Sr_2CaCu_2O_{8+\delta}$ *cuprate superconductors. Sci. Rep.* **2**, 248; DOI:10.1038/srep00248 (2012).